

Electronic Supplementary Information

Note Added After First Publication: This ESI file replaces the original version, first published on 27th November 2017. The authors regret that in the original version Fig. S8 (b), Page S12, the powder XRD patterns of simulated data and after MB adsorption were reversed.

Design of Two Isoreticular Cd-Biphenyltetracarboxylate Frameworks for Dye Adsorption, Separation and Photocatalytic Degradation

Wen-Juan Ji,^a Rui-Qing Hao,^a Wei- Wei Pei,^a Lin Feng,^a Quan-Guo Zhai^{b*}

^a. Key Laboratory of Magnetic Molecules & Magnetic Information Materials Ministry of Education,
School of Chemistry & Material Science, Shanxi Normal University,
Linfen, Shanxi, 041004, PR China

^b. Key Laboratory of Macromolecular Science of Shaanxi Province, School of Chemistry &
Chemical Engineering, Shaanxi Normal University, Xi'an,
Shaanxi, 710062, PR China

Thermal stability

To examine the stabilities of these two frameworks, TGA studies were carried out under N₂ atmosphere in the temperature range 25 – 900 °C (Fig. S10). As observed from TGA curve of **1**, there are loss half-coordinated H₂O and half-coordinated DMPU (found: 8.5% calcd. 9.4%) from 183 °C to 215 °C, then its coordinated two coordinated DMA molecules start to decompose thermally from 216 to 387 °C (found: 18.9% calcd. 20.2%). After that, the organic components start to decompose. Similarly, for **2**, there are loss four coordinated DMA, one coordinated H₂O and one free DMA (found: 30.1% calcd. 30.6%) from 25 to 232 °C. The second weight loss took place at around 328 °C was attributed to the destruction of the framework structure.

FT-IR spectra

As shown in Fig. S11, The IR spectra of compounds **1** and **2** have the strong and broad absorption bands in the range of 3000–3500 cm⁻¹ assigned as characteristic peaks of O-H, C-H and N-H vibrations. The stretching frequency for the carbonyl group on the benzene ring, normally in the range of 1680 – 1720 cm⁻¹, is lowered after coordination to the metal ion. Peaks at 1633 cm⁻¹ and 1385 cm⁻¹ could be assigned to the stretching vibration of carboxyl, the stretching vibration absorption peak around 1121 cm⁻¹ for the coordination of carbonyl. The peak of 771 cm⁻¹ could be considered to belong to out-of-plane bending vibration of C–H on benzene.

Table S1. Crystal data and structural refinements for compounds **1** and **2**.

Compounds	1	2
Empirical formula	C ₃₀ H ₃₇ Cd ₂ N ₄ O _{11.50}	C ₅₂ H ₆₁ Cd ₄ N ₅ O ₂₃
F _w	862.44	1573.66
Crys.Sys	monoclinic	Orthorhombic
Space group	P2 ₁ /n	Pbcn
a(Å)	14.3482(17)	27.0301(10)
b(Å)	13.7645(16)	19.4983(5)
c(Å)	18.792(2)	28.5432(8)
α(°)	90.00	90
β(°)	92.701(2)	90
γ(°)	90.00	90
V(Å ³)	3707.1(8)	15043.4(8)
Z	4	8
Density(Mg m ⁻³)	1.545	1.390
μ(mm ⁻¹)	1.206	1.181
F(000)	1372	6272
Crys.Size(mm)	0.41x0.40x0.36	0.42 x 0.40 x 0.35
θ(°)	2.29 to 25.02	3.16 to 25.02
Reflections	42060	46414
Data / restraints / parameters	6510 / 0 / 563	13252 / 0 / 772
Goodness-of-fit on F ²	1.106	1.067
R ₁ ^a , wR ₂ ^b [[I > 2σ(I)]]	0.0515, 0.1525	0.0523, 0.1534
R ₁ ^a , wR ₂ ^b (all data)	0.0586, 0.1646	0.0713, 0.1637
Δρ _{max} / Δρ _{min} (e Å ⁻³)	2.231 / -1.260	1.731 / -1.070

^a R₁ = F_o - F_c/F_o, wR₂ = [w(F_o² - F_c²)² / w(F_o²)²]^{1/2}

Table S2. Selected bonded lengths (\AA) and angles (deg) for compound **1**.

Cd(1)-O(1)	2.300(4)	Cd(1)-O(2)	2.379(5)	Cd(1)-O(3)	2.286(4)
Cd(1)-O(4)	2.538(5)	Cd(1)-O(5)	2.171(4)	Cd(1)-O(7)	2.213(4)
Cd(2)-O(3)	2.320(4)	Cd(2)-O(6)	2.270(5)	Cd(2)-O(8)	2.235(4)
Cd(2)-O(9)	2.290(5)	Cd(2)-O(10)	2.247(7)	Cd(2)-O(11)	2.292(6)
O(5)-Cd(1)-O(7)	95.2(2)	O(5)-Cd(1)-O(3)	107.96(17)	O(7)-Cd(1)-O(3)	99.09(15)
O(5)-Cd(1)-O(1)	100.96(17)	O(7)-Cd(1)-O(1)	105.48(19)	O(3)-Cd(1)-O(1)	139.83(16)
O(5)-Cd(1)-O(2)	155.59(17)	O(7)-Cd(1)-O(2)	98.8(2)	O(3)-Cd(1)-O(2)	89.47(16)
O(1)-Cd(1)-O(2)	56.02(16)	O(5)-Cd(1)-O(4)	91.20(19)	O(7)-Cd(1)-O(4)	153.02(16)
O(3)-Cd(1)-O(4)	54.10(14)	O(1)-Cd(1)-O(4)	98.93(18)	O(2)-Cd(1)-O(4)	85.3(2)
O(8)-Cd(2)-O(10)	91.9(3)	O(8)-Cd(2)-O(6)	97.1(2)	O(10)-Cd(2)-O(6)	96.3(3)
O(8)-Cd(2)-O(9)	86.1(2)	O(10)-Cd(2)-O(9)	86.9(3)	O(6)-Cd(2)-O(9)	175.4(2)
O(8)-Cd(2)-O(11)	171.5(2)	O(10)-Cd(2)-O(11)	89.7(3)	O(6)-Cd(2)-O(11)	91.0(2)
O(9)-Cd(2)-O(11)	85.7(3)	O(8)-Cd(2)-O(3)	86.37(18)	O(10)-Cd(2)-O(3)	172.2(2)
O(6)-Cd(2)-O(3)	91.45(16)	O(9)-Cd(2)-O(3)	85.4(2)	O(11)-Cd(2)-O(3)	90.9(2)

A) $-x + 1/2, y + 1/2, -z + 1/2$; B) $-x + 1/2, y - 1/2, -z + 1/2$; C) $-x + 1, -y, -z$; D) $x + 1/2, -y - 1/2, z + 1/2$; E) $x - 1/2, -y - 1/2, z - 1/2$; F) $-x + 3/2, y - 1/2, -z + 1/2$

Table S3. Selected bonded lengths (\AA) and angles (deg) for compound **2**.

Cd(1)-O(1)	2.238(5)	Cd(1)-O(7C)	2.523(5)	Cd(1)-O(8C)	2.295(4)
Cd(1)-O(11A)	2.341(5)	Cd(1)-O(12A)	2.346(5)	Cd(1)-O(16B)	2.190(5)
Cd(2)-O(2)	2.209(6)	Cd(2)-O(8C)	2.315(5)	Cd(2)-O(15B)	2.222(5)
Cd(2)-O(17)	2.234(7)	Cd(2)-O(21W)	2.227(9)	Cd(2)-O(22W)	2.312(8)
Cd(3)-O(3)	2.267(5)	Cd(3)-O(5D)	2.238(5)	Cd(3)-O(9)	2.309(7)
Cd(3)-O(18)	2.300(6)	Cd(3)-O(19)	2.311(5)	Cd(3)-O(20)	2.339(7)
Cd(4)-O(4)	2.177(5)	Cd(4)-O(6D)	2.213(5)	Cd(4)-O(9)	2.336(4)
Cd(4)-O(10)	2.403(5)	Cd(4)-O(13E)	2.352(5)	Cd(4)-O(14E)	2.315(4)
O(16B)-Cd(1)-O(1)	98.9(2)	O(16B)-Cd(1)-O(8C)	111.57(18)	O(1)-Cd(1)-O(8C)	94.72(16)
O(16B)-Cd(1)-O(11A)	148.42(17)	O(1)-Cd(1)-O(11A)	92.9(2)	O(8C)-Cd(1)-O(11A)	96.39(17)
O(16B)-Cd(1)-O(12A)	92.98(17)	O(1)-Cd(1)-O(12A)	108.2(2)	O(8C)-Cd(1)-O(12A)	143.47(19)
O(11A)-Cd(1)-O(12A)	55.45(16)	O(16B)-Cd(1)-O(7C)	97.2(2)	O(1)-Cd(1)-O(7C)	148.37(16)
O(8C)-Cd(1)-O(7C)	53.92(15)	O(11A)-Cd(1)-O(7C)	87.4(2)	O(12A)-Cd(1)-O(7C)	97.9(2)
O(2)-Cd(2)-O(15B)	97.8(2)	O(2)-Cd(2)-O(21)	88.1(3)	O(15B)-Cd(2)-O(21)	87.5(3)
O(2)-Cd(2)-O(17)	96.8(3)	O(15B)-Cd(2)-O(17)	164.1(3)	O(21W)-Cd(2)-O(17)	86.8(3)
O(2)-Cd(2)-O(22W)	168.6(3)	O(15B)-Cd(2)-O(22W)	90.8(3)	O(21W)-Cd(2)-O(22W)	99.8(4)
O(17)-Cd(2)-O(22W)	75.7(3)	O(2)-Cd(2)-O(8C)	82.93(19)	O(15B)-Cd(2)-O(8C)	90.92(19)
O(21)-Cd(2)-O(8C)	170.6(3)	O(17)-Cd(2)-O(8C)	97.1(3)	O(22)-Cd(2)-O(8C)	89.5(3)
O(5D)-Cd(3)-O(3)	96.0(2)	O(5D)-Cd(3)-O(18)	96.9(2)	O(3)-Cd(3)-O(18)	90.8(2)
O(5D)-Cd(3)-O(9)	86.48(18)	O(3)-Cd(3)-O(9)	96.54(17)	O(18)-Cd(3)-O(9)	171.6(2)
O(5D)-Cd(3)-O(19)	91.0(2)	O(3)-Cd(3)-O(19)	168.1(2)	O(18)-Cd(3)-O(19)	78.8(2)
O(9)-Cd(3)-O(19)	93.49(18)	O(5D)-Cd(3)-O(20)	170.5(2)	O(3)-Cd(3)-O(20)	89.4(2)
O(18)-Cd(3)-O(20)	90.9(3)	O(9)-Cd(3)-O(20)	85.1(2)	O(19)-Cd(3)-O(20)	85.1(2)
O(4)-Cd(4)-O(6D)	92.6(2)	O(4)-Cd(4)-O(14E)	95.32(18)	O(6D)-Cd(4)-O(14E)	116.0(2)
O(4)-Cd(4)-O(9)	105.60(19)	O(6D)-Cd(4)-O(9)	93.02(16)	O(14E)-Cd(4)-O(9)	143.48(17)
O(4)-Cd(4)-O(13E)	150.58(17)	O(6D)-Cd(4)-O(13E)	96.8(2)	O(14E)-Cd(4)-O(13E)	55.57(17)
O(9)-Cd(4)-O(13E)	101.70(18)	O(4)-Cd(4)-O(10)	96.6(2)	O(6D)-Cd(4)-O(10)	148.09(17)
O(14E)-Cd(4)-O(10)	93.58(19)	O(9)-Cd(4)-O(10)	55.08(15)	O(13E)-Cd(4)-O(10)	90.0(2)

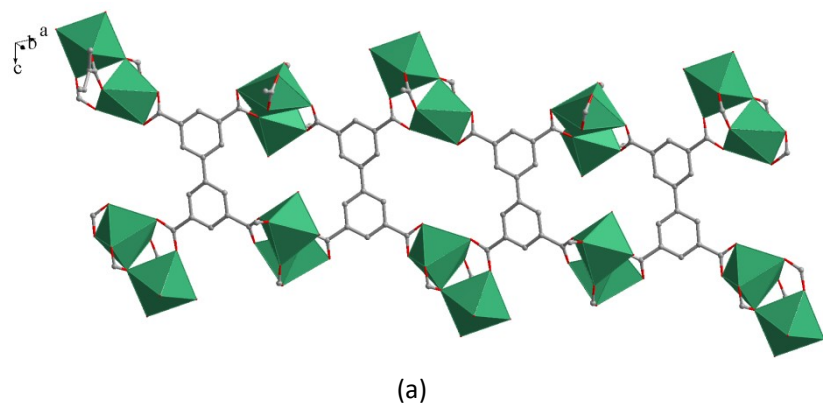
A). -x + 1, y, -z + 3/2; B) x, -y + 2, z - 1/2; C) -x + 1, -y + 1, -z + 1; D) -x + 3/2, y + 1/2, z; E) -x + 3/2, y - 1/2, z;

Table S4. Pseudo-second-order kinetics parameters for MB adsorb into **1** and **2**.

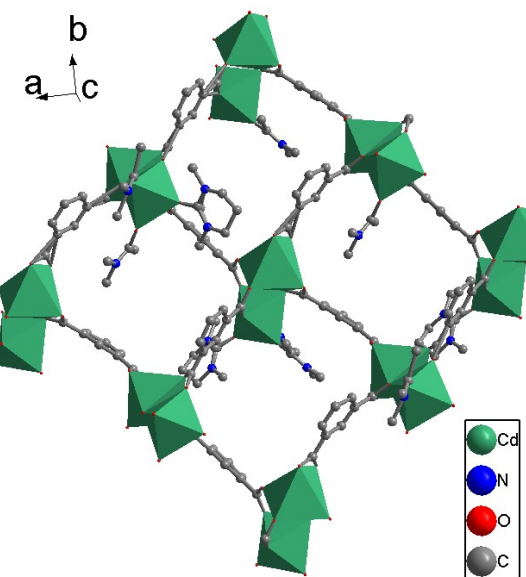
Absorbent	q_e (mg g ⁻¹)	K^2 (g mg ⁻¹ h ⁻¹)	R^2
1	12.8	0.014261	0.9927
	16.0	0.011936	0.9905
	19.2	0.011679	0.9925
	22.4	0.011249	0.9973
	32.0	0.005348	0.9912
2	12.8	0.053275	0.9987
	16.0	0.038666	0.9995
	19.2	0.036718	0.9983
	22.4	0.035905	0.9975
	32.0	0.018344	0.9973

Table S5. Langmuir model of MOF **1** or **2** adsorption for MB.

Absorbent	Dye	K_L /L mg ⁻¹	q_m / mg g ⁻¹	R^2
1	MB	0.21	72.99	0.9920
2	MB	12.6	79.36	0.9973



(a)



(b)

Fig. S1. (a) The large 22-membered $[Cd_2C_{16}O_4]$ metal-organic rings. (b) Schematic views of the 2D layer for **1**.

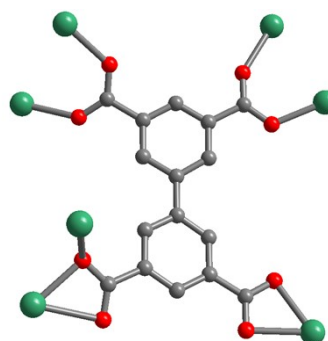


Fig. S2. The coordination fashion of carboxylate groups for **1**.

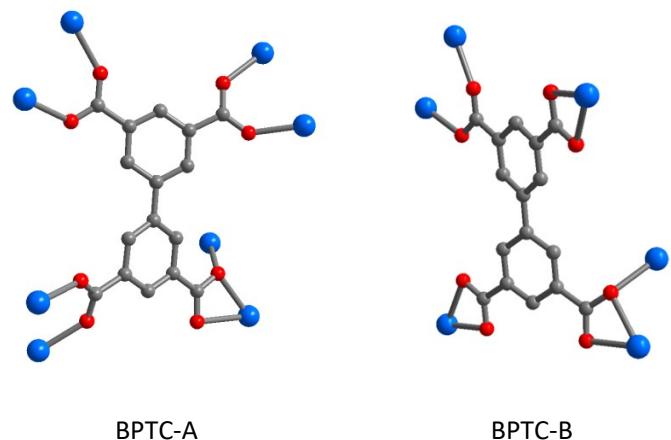


Fig. S3. The coordination fashion of carboxylate groups for **2**.

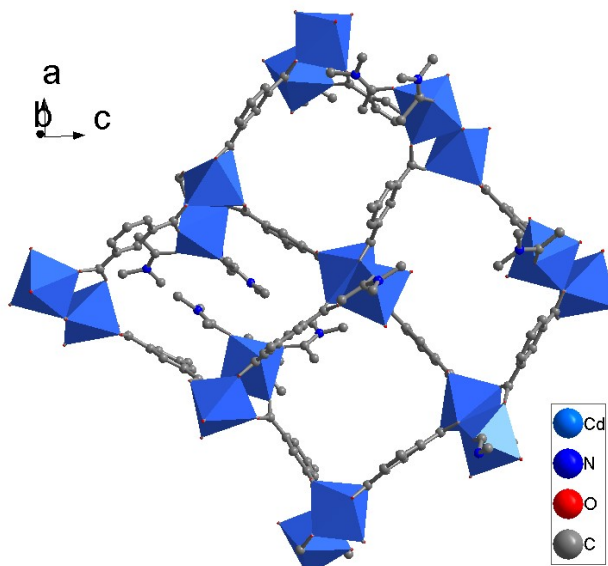


Fig. S4. Schematic views of the 2D layer for **2**.

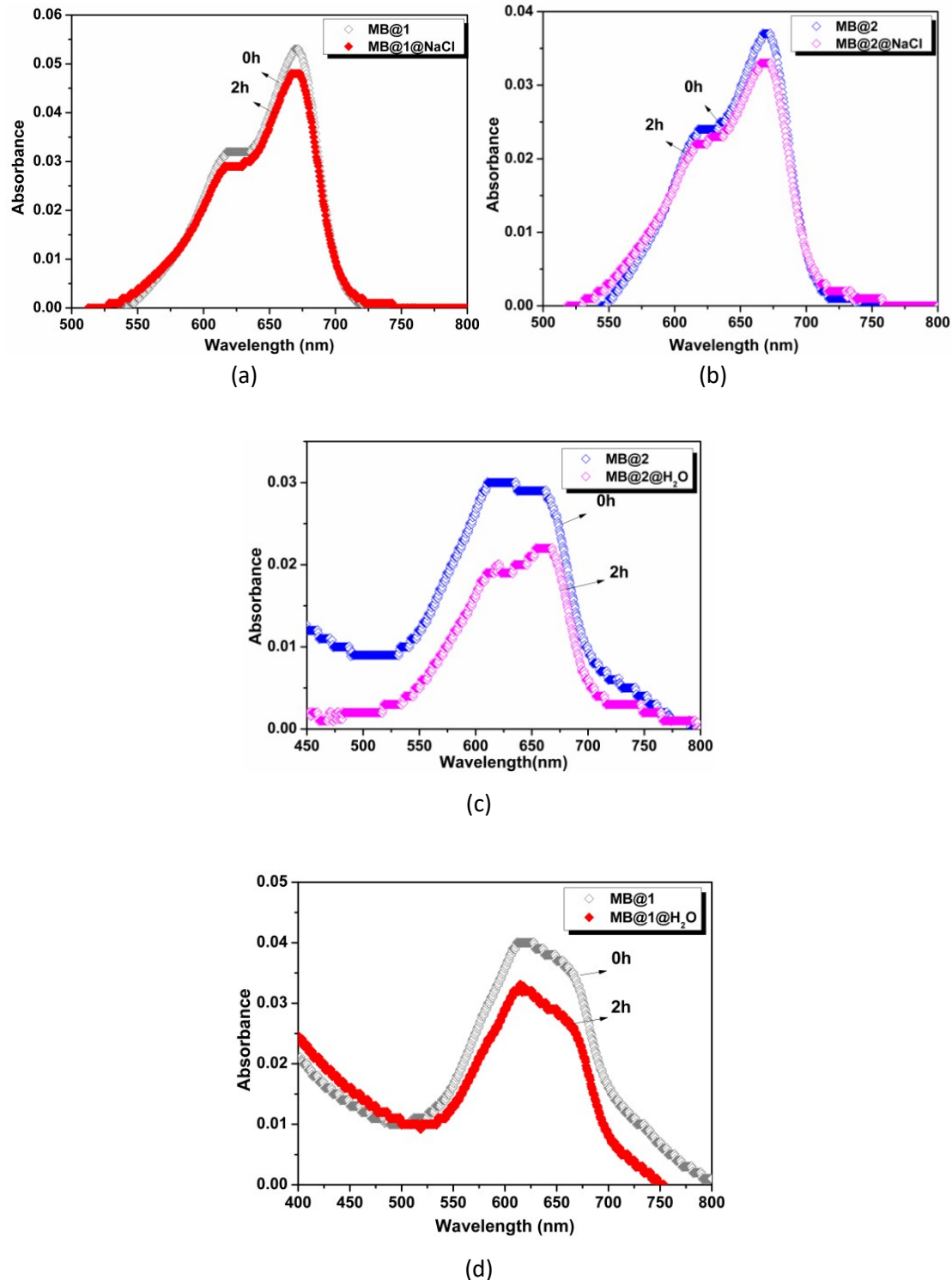


Fig. S5. The UV-vis absorption spectra of MB@1 or MB@2 in saturated NaCl solution (a and b) and deionized water (c and d).

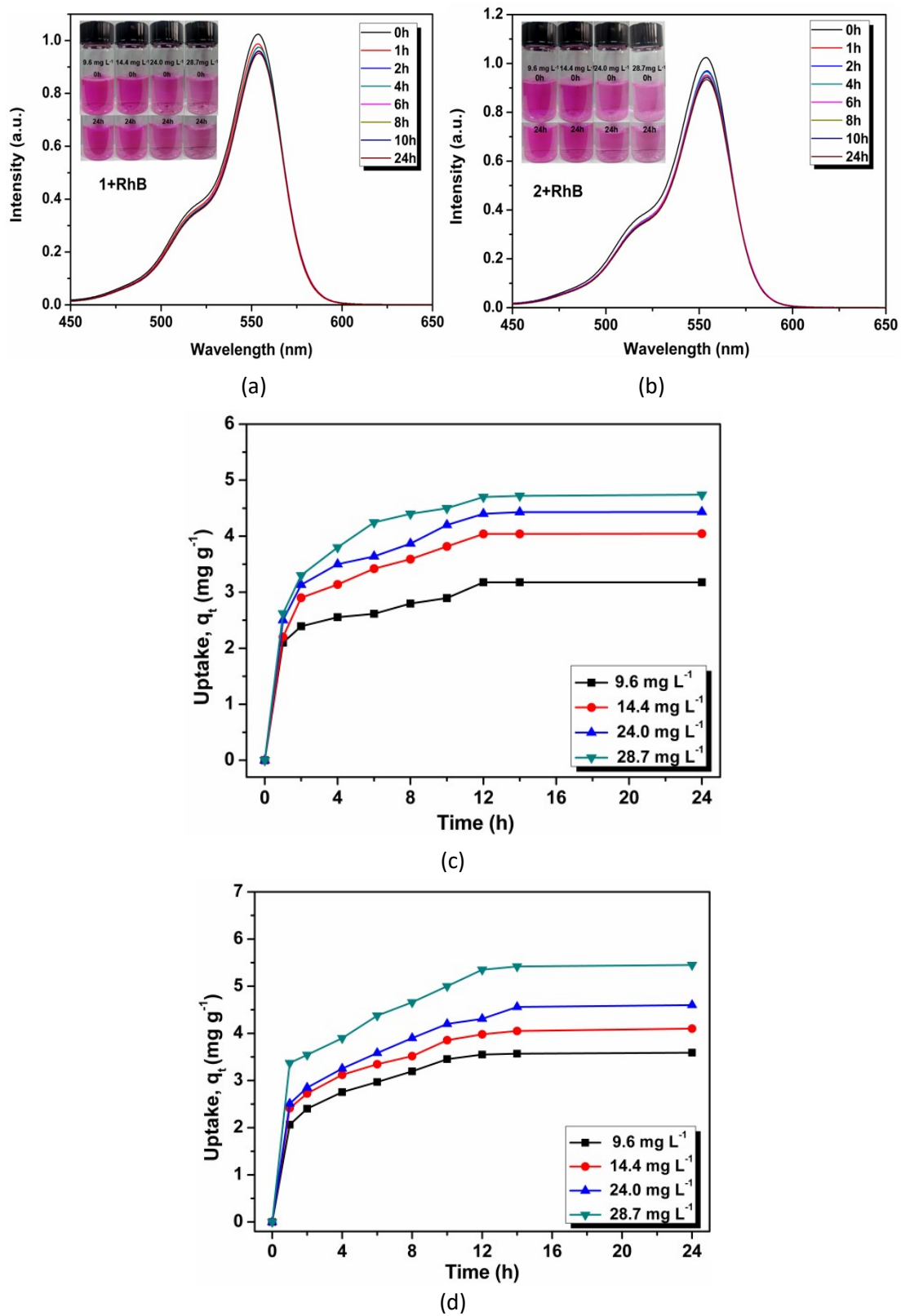
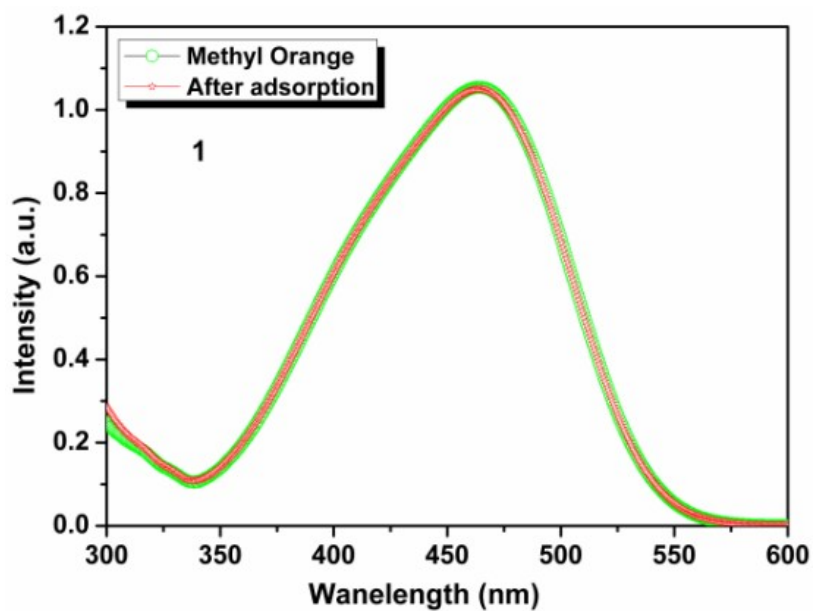
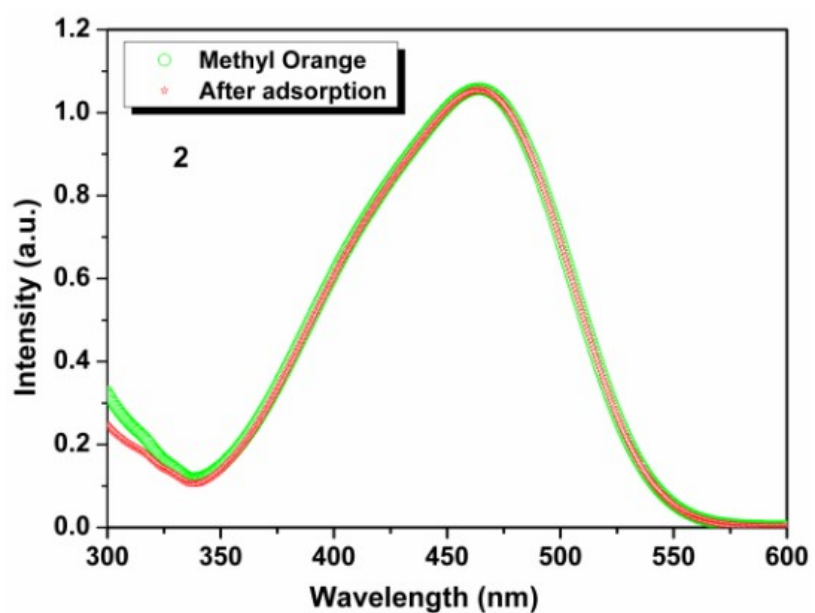


Fig. S6. Sequential UV-Vis spectra of RhB in aqueous solution after addition of MOFs (a and b) and the adsorption capacity of RhB for two MOFs (c - 1 and d - 2).

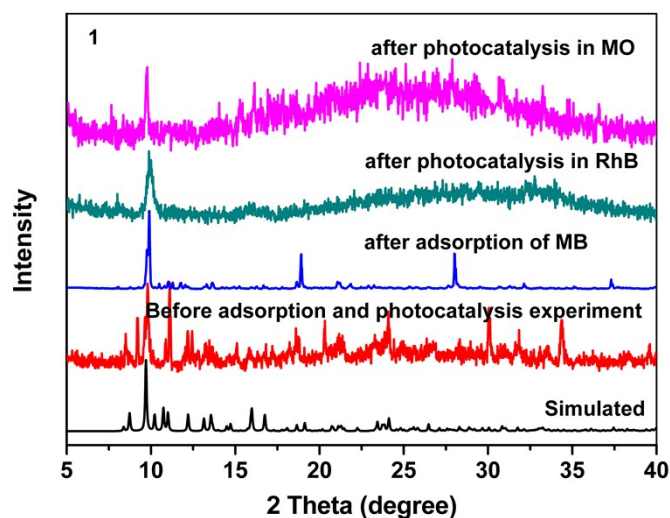


(a)

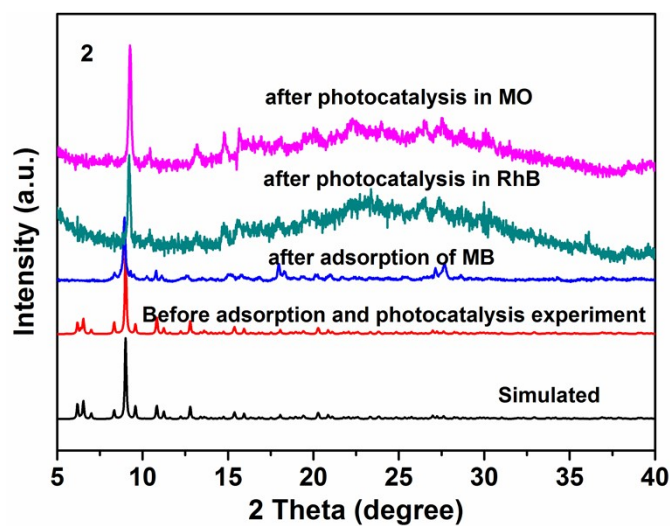


(b)

Fig. S7. UV-vis absorption spectra of the pure MO solution and with MOFs **1** (a) and **2** (b).



(a)



(b)

Fig. S8. The simulated, before experimental and after adsorption and photocatalysis reaction powder XRD patterns for **1** (a) and **2** (b).

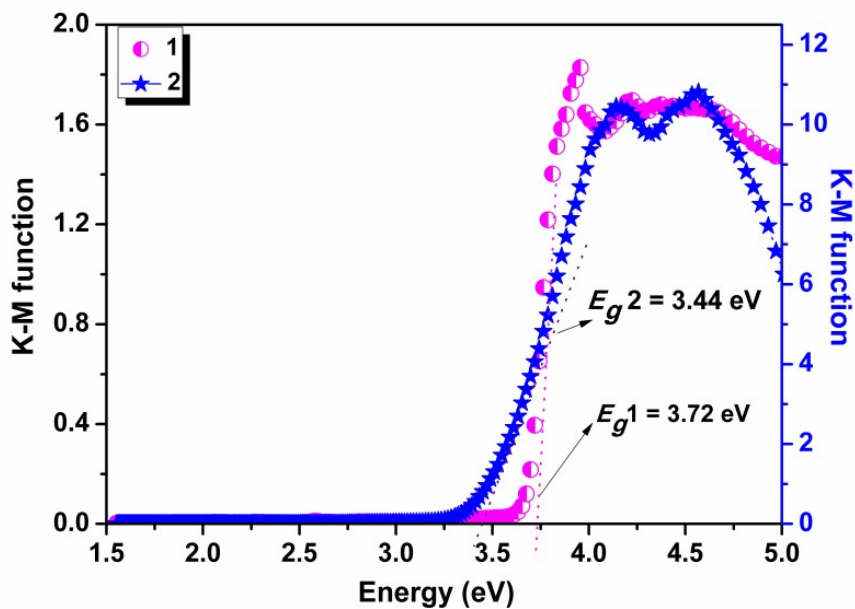


Fig. S9. The UV-vis diffuse reflectance data for **1** and **2**.

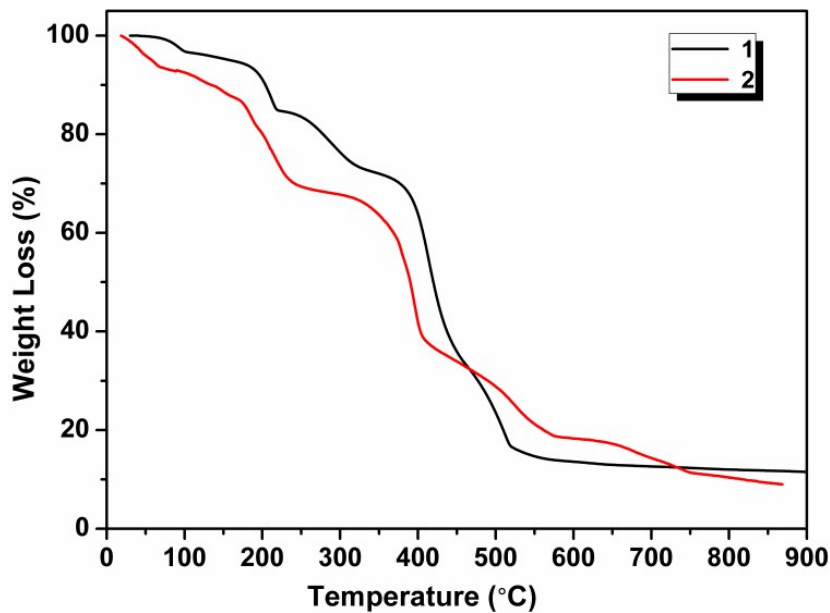


Fig. S10. Thermogravimetric curves for **1** and **2**.

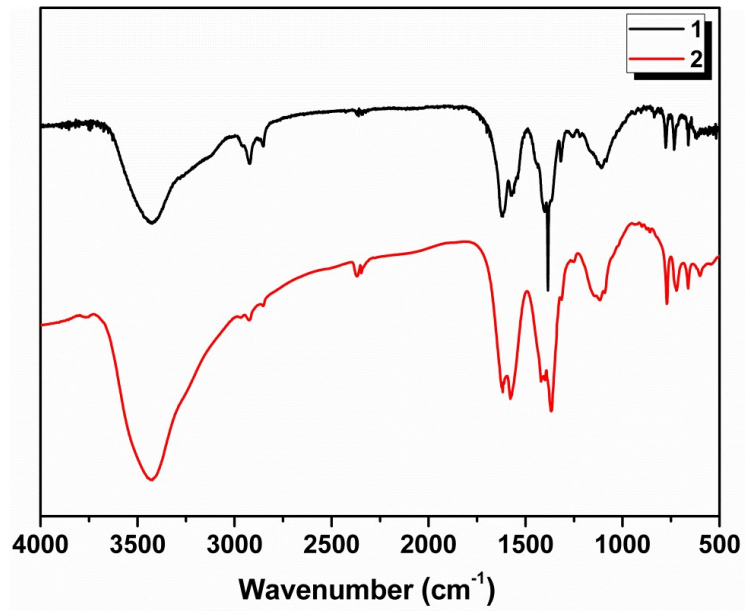


Fig. S11. FT-IR spectra of compounds **1** and **2**.